

5 Optical Fibers

Takis Hadjifotiou
Telecommunications Consultant

Introduction

Optical fiber communications have come a long way since Kao and Hockman (then at the Standard Telecommunications Laboratories in England) published their pioneering paper on communication over a piece of fiber using light (Kao & Hockman, 1966). It took Robert Maurer, Donald Keck, and Peter Schultz (then at Corning Glass Works–USA) four years to reach the loss of 20 dB/km that Kao and Hockman had considered as the target for loss, and the rest, as they say, is history. For those interested in the evolution of optical communications, Hecht (1999) will provide a clear picture of the fiber revolution and its ramifications.

The purpose of this chapter is to provide an outline of the performance of fibers that are fabricated today and that provide the pathway for the transmission of light for communications.

The research literature on optical fibers is vast, and by virtue of necessity the references at the end of this chapter are limited to a few books that cover the topics outlined here.

The Structure and Physics of an Optical Fiber

The optical fibers used in communications have a very simple structure. They consist of two sections: the glass core and the cladding layer (Figure 5.1).

The core is a cylindrical structure, and the cladding is a cylinder without a core. Core and cladding have different refractive indices, with the core having a refractive index, n_1 , which is slightly higher than that of the cladding, n_2 . It is this difference in refractive indices that enables the fiber to guide the light. Because of this guiding property, the fiber is also referred to as an “optical waveguide.” As a minimum there is also a further layer known as the secondary cladding that does not participate in the propagation but gives the fiber a minimum level of protection. This second layer is referred to as a coating.

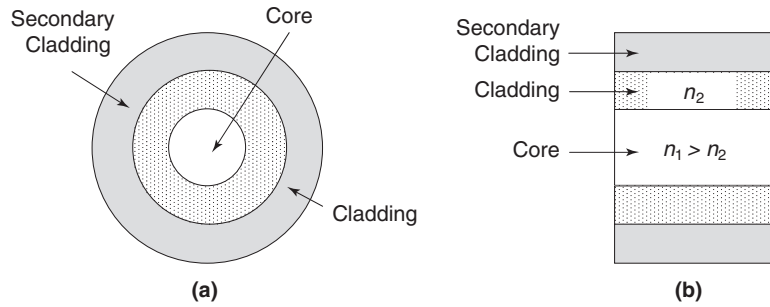


Fig. 5.1 (a) Cross section and (b) longitudinal cross section of a typical optical fiber.

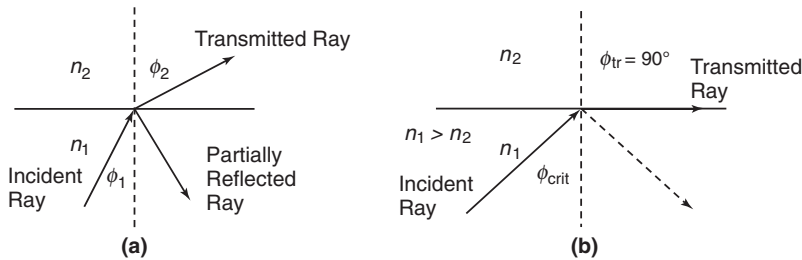


Fig. 5.2 Snell's law.

The basics of light propagation can be discussed with the use of geometric optics. The basic law of light guidance is Snell's law (Figure 5.2a). Consider two dielectric media with different refractive indices and with $n_1 > n_2$ and that are in perfect contact, as shown in Figure 5.1. At the interface between the two dielectrics, the incident and refracted rays satisfy Snell's law of refraction—that is,

$$n_1 \sin \phi_1 = n_2 \sin \phi_2 \quad (5.1)$$

or

$$\frac{\sin \phi_1}{\sin \phi_2} = \frac{n_2}{n_1} \quad (5.2)$$

In addition to the refracted ray there is a small amount of reflected light in the medium with refractive index n_1 . Because $n_1 > n_2$ then always $\phi_2 > \phi_1$. As the angle of the incident ray increases there is an angle at which the refracted ray emerges parallel to the interface between the two dielectrics (Figure 5.2(b)).

This angle is referred to as the critical angle, ϕ_{crit} , and from Snell's law is given by

$$\sin \phi_{\text{crit}} = \frac{n_2}{n_1} \quad (5.3)$$

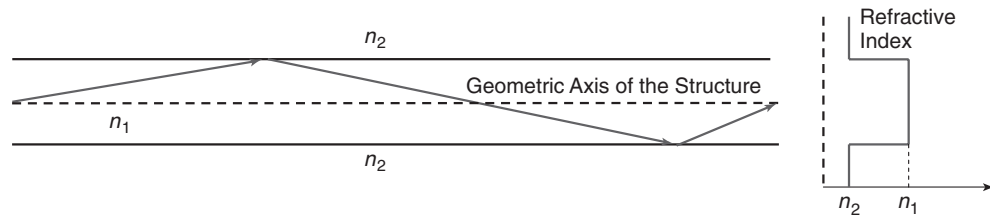


Fig. 5.3 Light guidance using Snell's law.

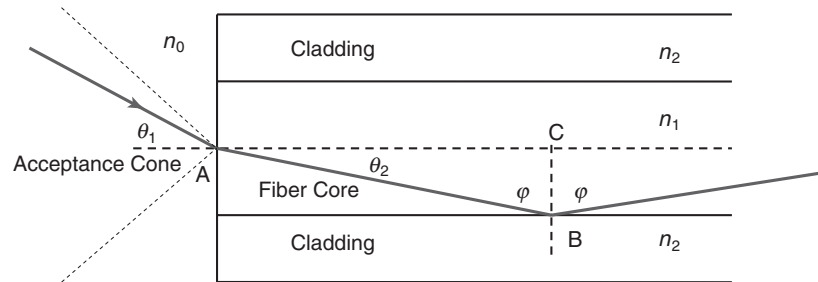


Fig. 5.4 Geometry for the derivation of the acceptance angle.

If the angle of the incident ray is greater than the critical angle, the ray is reflected back into the medium with refractive index n_1 . This basic idea can be used to propagate a light ray in a structure with $n_1 > n_2$, and Figure 5.3 illustrates this idea.

The light ray incident at an angle greater than the critical angle can propagate down the waveguide through a series of total reflections at the interface between the two dielectrics. The ray shown in Figure 5.3 is referred to as a “meridional ray” because it passes through the axis of the fiber. For rays not satisfying this condition, see Senior (1992). Clearly, the picture of total internal reflection assumes an ideal situation without imperfections, discontinuities, or losses. In a real-world fiber, imperfections will introduce light that is refracted as well as reflected at the boundary. In arriving at the basic idea of light propagation, it was assumed that somehow the ray has been launched into the fiber.

For a ray to be launched into the fiber and propagated it must arrive at the interface between the two media (with different refractive indices) at an angle that is at minimum equal to ϕ_{crit} and in general less than that. Figure 5.4 illustrates the geometry for the derivation of the acceptance angle. To satisfy the condition for total internal reflection, the ray arriving at the interface, between the fiber and outside medium, say air, must have an angle of incidence less than θ_{acc} , otherwise the internal angle will not satisfy the condition for total reflection, and the energy of the ray will be lost in the cladding.

Consider that a ray with an incident angle less than the θ_{acc} , say θ_1 , enters the fiber at the interface of the core (n_1) and the outside medium, say air (n_0), and the ray lies in the meridional plane. From Snell's law at the interface we obtain

$$n_0 \sin \theta_1 = n_1 \sin \theta_2 \quad (5.4)$$

From the right triangle ABC (Figure 5.4), the angle ϕ is given by

$$\phi = \frac{\pi}{2} - \theta_2 \quad (5.5)$$

where the angle ϕ is greater than the critical angle. Substituting equation 5.5 into equation 5.4 we obtain

$$n_0 \sin \theta_1 = n_1 \cos \phi \quad (5.6)$$

In the limit as the incident angle, θ_1 , approaches θ_{acc} , the internal angle approaches the critical angle for total reflection, ϕ_{crit} . Then, by introducing the trigonometric relation $\sin^2 \phi + \cos^2 \phi = 1$ into equation 5.4, we obtain

$$n_0 \sin \theta_1 = n_1 \cos \phi = n_1 (1 - \sin^2 \phi)^{1/2} = n_1 \left(1 - \left(\frac{n_2}{n_1} \right)^2 \right)^{1/2} = (n_1^2 - n_2^2)^{1/2} \quad (5.7)$$

This equation defines the angle within which the fiber can accept and propagate light and is referred to as the “Numerical Aperture” (NA).

$$\text{NA} = n_0 \sin \theta_{\text{acc}} = (n_1^2 - n_2^2)^{1/2} \quad (5.8)$$

When the medium with refractive index n_0 is air, the equation for the NA of the glass fiber simplifies to

$$\text{NA} = \sin \theta_{\text{acc}} = (n_1^2 - n_2^2)^{1/2} \quad (5.9)$$

This equation states that for all angles of incident where the inequality $0 \leq \theta_1 \leq \theta_{\text{acc}}$ is satisfied the incident ray will propagate within the fiber. The parameter NA expresses the propensity of the fiber to accept and propagate light within the solid cone defined by an angle, $2\theta_{\text{acc}}$. The equation for the NA can be also expressed in terms of the difference between the refractive indices of core and cladding—that is,

$$\Delta = \frac{n_1^2 - n_2^2}{2n_1^2} \approx \frac{n_1 - n_2}{n_1} \quad (5.10)$$

With these simplifications the NA can now be written as

$$\text{NA} = n_1 (2\Delta)^{1/2} \quad (5.11)$$

To appreciate the numbers involved, consider a fiber made of silica glass whose core refractive index is 1.5 and that of the cladding is 1.46. The ϕ_{crit} and the NA of the fiber are calculated to be

$$\begin{aligned} \phi_{\text{crit}} &= \sin^{-1} \left(\frac{n_2}{n_1} \right) = \sin^{-1} \left(\frac{1.46}{1.50} \right) = 76.73^\circ \\ \text{NA} &= (n_1^2 - n_2^2)^{1/2} = (1.50^2 - 1.46^2)^{1/2} = (2.25 - 2.13)^{1/2} = 0.346 \\ \theta_{\text{acc}} &= \sin^{-1} \text{NA} = \sin^{-1} 0.346 = 20.24^\circ \end{aligned}$$

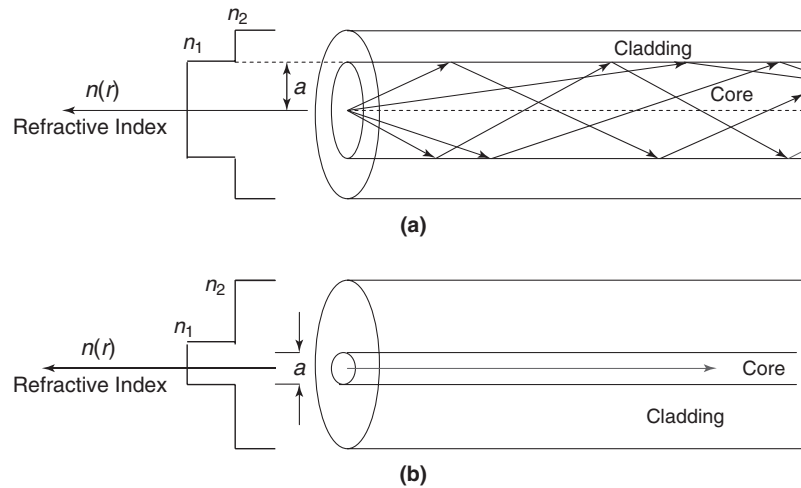


Fig. 5.5 (a) Multimode and (b) single-mode propagation for step index fiber.

If one uses the equation for the approximation of NA, equation 5.11, the result is

$$\text{NA} \approx n_1(2\Delta)^{1/2} = 1.5 \times \left(2 \times \left(\frac{1.50 - 1.46}{1.5} \right) \right)^{1/2} = 1.5 \times (2 \times 0.0266)^{1/2} = 0.346$$

If the ray does not lie in the meridional plane, the analysis for obtaining the NA is slightly more complex.

The discussion up to now has been based on the launching and propagation of a single ray. Because all the rays with a reflection angle less than the critical angle can propagate, it is expected that a number of rays will propagate provided they can be launched into the fiber. The class of fiber that can support the simultaneous propagation of a number of rays is known as multimode fiber. The term “mode” is used in a more sophisticated analysis of light propagation using Maxwell’s equations, and it corresponds to one solution of the equations. Therefore, the concept of a ray and a mode are equivalent, and in the rest of this chapter the term “mode” will be used.

A fiber that allows the propagation of one mode only is called a single-mode fiber. A fiber can be multimode or single mode, and the behavior depends on the relative dimensions of the core and the wavelength of the propagating light. Fibers with a core diameter much larger than the wavelength of the launched light will support many propagating modes, and the propagating conditions can be analyzed with geometric optics. A fiber with a core diameter similar to that of the light wavelength supports only one propagation mode. Figure 5.5 illustrates these concepts.

Material Characteristics of Fibers—Losses

The basic material used in the manufacture of optical fiber for optical transmission is silica glass. A large number of glasses have been developed and studied with the objective of improving fiber transmission properties. There are two parameters of glass that have a substantial impact on its performance: the losses and the changes of refractive index with

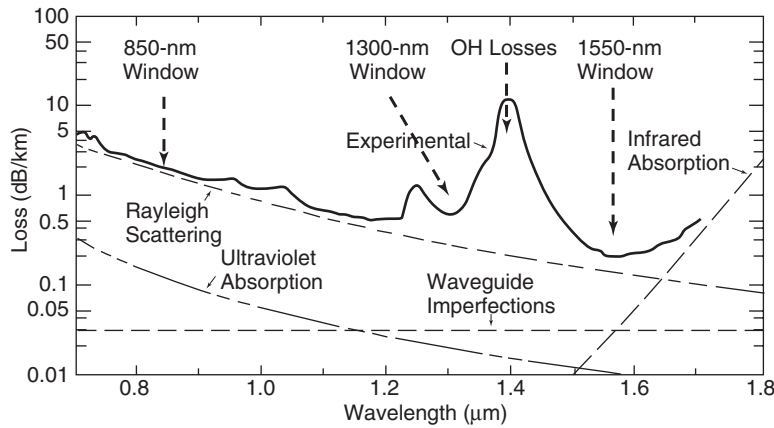


Fig. 5.6 Measured loss versus wavelength for SiO_2 fibers. *Source:* Adapted from Hecht (1999). Used with permission.

wavelength. The basic material used in the manufacture of optical fibers is vitreous silica dioxide (SiO_2), but to achieve the properties required from a fiber, various dopants are also used, (Al_2O_3 , B_2O_3 , GeO_2 , P_2O_5). Their task is to slightly increase and decrease the refractive index of pure silica (SiO_2). Initially the fiber losses were high, but through improvements in the quality of the materials and the actual production process, the losses have been reduced so as to be close to the theoretical expected losses.

In the part of the electromagnetic spectrum where optical fiber transmission takes place, the losses are bracketed between two asymptotes: ultraviolet absorption and infrared absorption. The measured loss-versus-wavelength curve is shown in Figure 5.6.

The actual loss in the window between 0.8 and 1.6 μm is dictated by the Rayleigh scattering losses. The physical origin of the Rayleigh scattering losses is the excitation and re-radiation of the incident light by atomic dipoles whose dimensions are much less than the wavelength of the light. The loss can be expressed in terms of decibels per kilometer by the expression

$$\alpha_{\text{scat}} = \frac{A_R}{\lambda^4} \quad (5.12)$$

Where the constant A_R reflects the details of the doping process and the fiber fabrication, and the value of A_R is around $0.95 \text{ dB/km} - \mu\text{m}^4$. In fiber with a pure silica core, the value of A_R can be as low as $0.75 \text{ dB/km} - \mu\text{m}^4$. The actual scattering within a fiber is higher than in that of bulk material because of additional scattering from interfaces and inhomogeneities in the fiber structure.

The losses discussed up to now are usually referred to as intrinsic because their origin is in the physical properties of the material. The total intrinsic loss can be expressed as the sum of the three—that is,

$$\alpha_{\text{intrinsic}} = \alpha_{\text{ultraviolet}} + \alpha_{\text{infrared}} + \alpha_{\text{scat}} \quad (5.13)$$

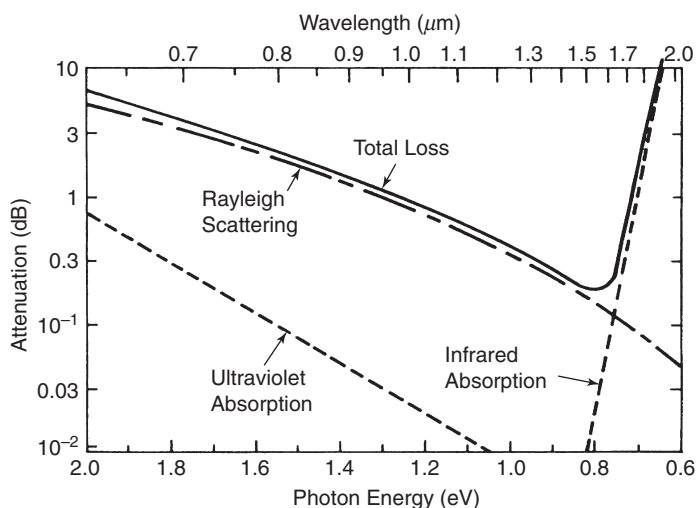


Fig. 5.7 Theoretical intrinsic loss characteristics of germania-doped silica ($\text{GeO}_2\text{-SiO}_2$) glass. Source: Adapted from Senior (1992). Used with permission.

The theoretical intrinsic loss has a minimum value of 0.185 dB/km at a wavelength close to 1550 nm. Figure 5.7 summarizes the intrinsic theoretical losses of a silica glass fiber.

In addition to the intrinsic losses, the fiber has additional losses that are referred to as extrinsic. These are associated with the presence of various substances in the glass, the quality of the glass, the processing, and the mechanical imperfections associated with the fiber structure.

These losses can be removed with refinements in the fabrication process and in the quality of glass. The presence of metallic and rare-earth impurities contributes to the extrinsic fiber loss as does the presence of the hydroxyl group OH that enters the glass through water vapors. These contributors to the extrinsic loss are the most difficult to remove (see Figure 5.6).

Another contributor to the extrinsic losses is the micro-bending and macro-bending of the fiber that arises from periodic microbends as a result of the spooling or cabling of the fiber and the bending of the fiber for cabling and deployment (Senior, 1992; Buck, 2004).

When the intrinsic and extrinsic losses are combined, the total fiber loss is as shown in Figure 5.6. The experimental results shown there are from the early 1980s, and the fiber of today has a loss that is very close to the intrinsic loss of the material. This was achieved by removing the OH extrinsic loss and improving the quality of the glass. The total loss of a modern fiber is shown in Figure 5.8.

The evolution of fiber in terms of loss generates three optical windows. The first window was around 850 nm with multimode fiber. The reason for operating at 850 nm was the availability of semiconductor lasers at this wavelength. When the silica zero-dispersion wavelength at 1300 nm was identified, the first single-mode systems operated at 1300 nm, the second window.

When it was possible to reduce the losses at the minimum-loss wavelength, 1550 nm, then single-mode systems started operating at 1550 nm, the third window. Long-haul systems operate in the region of 1550 nm either with a single wavelength or with multiple wavelengths (wavelength division multiplexing—see Chapter 6). The 1300-nm window is still used for short-haul systems.

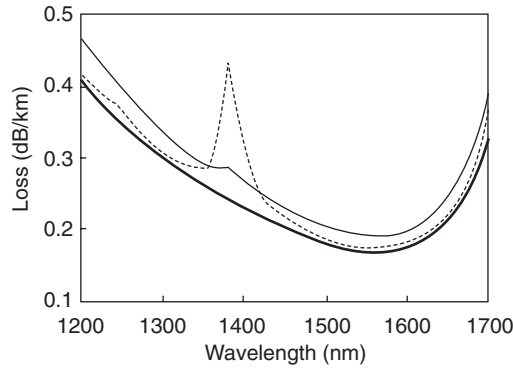


Fig. 5.8 Spectral loss of water loss free PSCF.

Source: Adapted from Chigusa et al. (2005). Used with permission.

— Water loss free PSCF
 - - - Conventional PSCF
 — Conventional G.652D fiber
 PSCF = Pure Silica Core Fiber

Material Characteristics of Fibers—Dispersion

The variation of refractive index of a material with wavelength is known in optics as dispersion, and it is responsible for resolution of white light into its constituent colors. In the context of fiber light propagation, the dispersion can be divided into two parts. The first part is the dispersion induced on the light by the material used in the waveguide, and this is known as material dispersion. The second part is the impact of the actual waveguide structure, and it is known as waveguide dispersion. This section will address material dispersion only (Senior, 1992; Buck, 2004).

The speed of propagation of monochromatic light in an optical fiber is given by the simple equation

$$u_{\text{phase}} = \frac{c}{n_1(\lambda)} \quad (5.14)$$

This speed is the phase velocity of the light wave, and it is different for each wavelength.

In transmitting a pulse of light through the fiber, the pulse can be expressed as the summation of a number of sine and cosine functions, which is known as the spectrum of the pulse. If the spectrum is centered on a frequency, ω , and has a small spectral width around ω , then a velocity can be associated with this group of frequencies, and this is known as the group velocity.

In conformity with the idea of velocity of propagation for monochromatic radiation, a group index can be defined as corresponding to the group of frequencies around ω . From a detailed analysis of propagation, group velocity is defined by

$$u_{\text{group}} = \frac{c}{n_1 - \lambda(dn_1/d\lambda)} = \frac{c}{N} \quad (5.15)$$

where the group index, N , of the material is defined as

$$N \equiv n_1 - \lambda \frac{dn_1}{d\lambda} \quad (5.16)$$

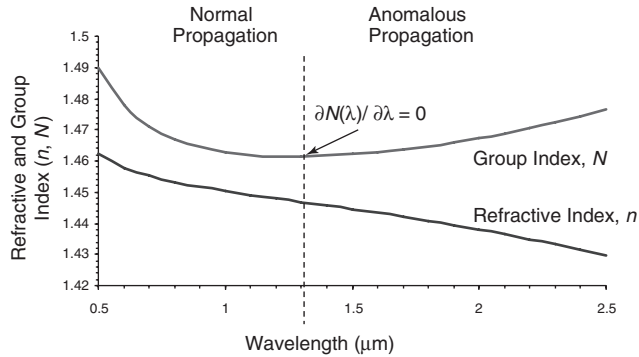


Fig. 5.9 Refractive index and group index for SiO₂ glass.

The packet of frequencies corresponding to the pulse will arrive at the output of the fiber sometime after the pulse is launched. This delay is the group delay, and it is defined as

$$\tau_g = \frac{L}{c} \left(n_1 - \lambda \frac{dn_1}{d\lambda} \right) = \frac{L}{c} \cdot N \quad (5.17)$$

where L is the fiber length. Figure 5.9 shows the refractive index and group index of SiO₂ glass fiber.

For any material, the zero group dispersion is the wavelength at which the curve of the refractive index has an inflection point. For silica this wavelength is at 1300 nm, and it is known as λ_0 . From Figure 5.9 one can distinguish two regions associated with the group index curve. The first region is the region with wavelengths less than λ_0 . In this region the group index decreases as the wavelength increases. This means that the spectral components of longer wavelength of the pulse travel faster than spectral components of shorter wavelengths. This regime is identified as the normal group dispersion regime and imposes a positive chirp. For wavelengths greater than λ_0 the opposite behavior is observed, and the region is identified as the anomalous group dispersion regime and a negative chirp is imposed on the pulse (Buck, 2004; Agrawal, 2001).

When measurements of these parameters are considered, it is useful to define a new parameter known as the material dispersion parameter, $D_m(\lambda)$. This parameter is defined as

$$D_m(\lambda) \equiv \frac{d(\tau_g/L)}{d\lambda} = \frac{1}{c} \cdot \frac{dN}{d\lambda} \quad (5.18)$$

where $D_m(\lambda)$ is expressed as picoseconds per nanometer of source bandwidth per kilometer of distance (ps/nm-km). Figure 5.10 shows the material dispersion of a pure silica glass fiber.

There are two ways to write in the time domain the spread of a pulse whose spectrum is centered at λ_s . For pulses without initial chirp, the change in pulse width is

$$\Delta\tau_m = -\Delta\lambda_{\text{width}} D_m(\lambda_s) L \quad (5.19)$$

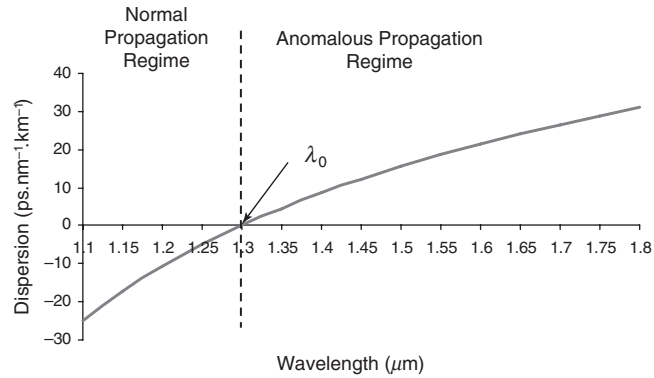


Fig. 5.10 Material (chromatic) dispersion of pure silica.

and in terms of the r.m.s. (Root Mean Square) width

$$\sigma_m = -\sigma_\lambda D_m(\lambda_s)L \quad (5.20)$$

where σ_λ is the r.m.s. width of the optical source. The value of λ_0 depends weakly on the dopants used in the fiber. For example, the use of 13.5 percent of GeO_2 shifts the λ_0 by 0.1 nm with respect to the λ_0 of pure SiO_2 . The material dispersion is also referred to as the chromatic dispersion.

Multimode Fibers

As explained in the section titled The Structure and Physics of an Optical Fiber, a multimode fiber can support the propagation of a number of modes (rays). Each of these modes carries the signal imposed on the optical wave. When the modes arrive at the receiver, they create a multi-image of the pulse launched in the waveguide. This multi-image can force the receiver to make a wrong decision regarding the transmitted bit of information.

Before we discuss this feature of multimode transmission, we will first look at the loss of multimode fibers (Senior, 1992).

The loss of multimode fibers should not be different from the spectral loss presented in Figure 5.8 because it is a question of material and processing. However, some manufacturers make available fiber that still has a higher loss, around 1380 nm, but far less loss than that shown in Figure 5.6. The reason for this is the high cost of completely eradicating the residual loss at the OH wavelength. In Figure 5.11 the spectral loss of a multimode fiber is shown; it is important to notice that the loss at the OH wavelength is only around 0.5 dB, compared to 10 dB shown in Figure 5.6.

Light propagating in a multimode fiber is subject to the material dispersion of the fiber. However, there is another form of dispersion that is specific to multimode fibers. Consider a step index multimode fiber with two propagating modes (Figure 5.12).

The first is the axial mode that propagates along the geometric axis of the fiber. The time taken by this mode to reach the end of the fiber is the minimum possible and the output is delayed by that time, which is given by Senior (1992) and Buck (2004):

$$\tau_{\min} = n_1 \frac{L}{c} \quad (5.21)$$

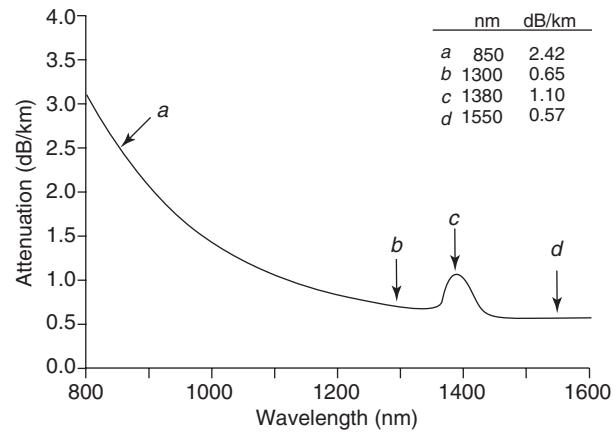


Fig. 5.11 Typical spectral loss for multimode fiber. Notice the low loss at the OH wavelength.
Source: Corning Inc.

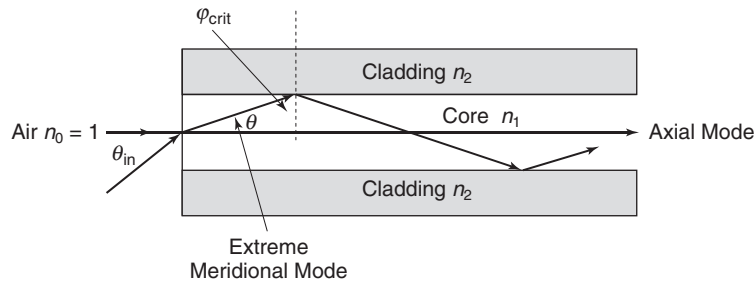


Fig. 5.12 Optical paths of meridional and axial modes.

where the symbols have their usual meaning. Now the extreme meridional mode will reach the output of the fiber after a delay that in this particular geometric arrangement will be the maximum and given by

$$\tau_{\max} = \frac{n_1}{c} \cdot \frac{L}{\cos\theta} \quad (5.22)$$

From Snell's law (equations 5.3 and 5.6), we have for the critical angle at the core-cladding interface the following equation:

$$\cos\theta = \sin\phi_{\text{crit}} = \frac{n_2}{n_1} \quad (5.23)$$

Then, substituting into equation 5.22 for $\cos\theta$,

$$\tau_{\max} = \frac{n_1^2}{n_2} \cdot \frac{L}{c} \quad (5.24)$$

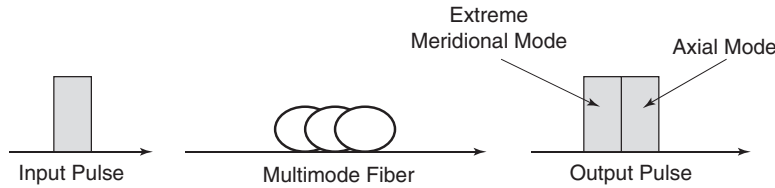


Fig. 5.13 Impact of the multimode fiber delay on the pulse output for a delay equal to the pulse width.

The difference in the delay between the two modes is given by

$$\Delta\tau_s \approx \Delta \frac{Ln_1}{c} \approx (\text{NA})^2 \cdot \frac{L}{2cn_1} \quad (5.25)$$

where NA stands for the numerical aperture of the fiber and Δ is given by equation 5.10. The r.m.s. broadening of the pulse is given by

$$\sigma_{s|\text{step}} \approx \Delta \frac{Ln_1}{2\sqrt{3}c} \approx (\text{NA})^2 \cdot \frac{L}{4\sqrt{3}cn_1} \quad (5.26)$$

To appreciate the impact of this differential delay, let us assume that a pulse of nominal width T is launched into the fiber. If the differential delay is equal to the pulse width, the output consists of two pulses occupying a total width of $2T$. This is illustrated in Figure 5.13.

The receiver will therefore detect two pulses when only one was sent. This effect is called the intermodal dispersion of the fiber, and it is an additional dispersion imparted on the pulse. There are a number of reasons why one has to be cautious in using equation 5.25 for long-haul communications.

The first is that equation 5.25 is a worst-case scenario. In an actual fiber, the power between adjacent modes is coupled back and forth, which leads to a partial mode delay equalization. The second is related to the physics of propagation. Modes that are weakly confined in the core spread out in the cladding, and if they meet higher loss than in the core, then the number of modes propagating is limited to those strongly confined in the core. The additional loss might be present in the cladding because the material used has a higher intrinsic loss or some of the modes might be radiated into the secondary cladding. These two effects limit the spread of the delay per mode, reducing the intermodal dispersion. In addition to pure fiber effects, there is another source of unpredictability in the mode structure of the light source and its statistics, leading to modal noise (Epworth, 1978).

To appreciate the quantities involved, consider a multimode step index fiber of 10 km length with a core refractive index of 1.5 and $\Delta = 2\%$. Then from equation 5.26 the r.m.s. pulse broadening is

$$\sigma_{s|\text{step}} = \Delta \frac{L \times n_1}{2\sqrt{3} \times c} = 0.02 \frac{10 \times 10^3 \times 1.5}{2\sqrt{3} \times 2.998 \times 10^8} = 2.88 \times 10^{-2} \frac{\text{ns}}{\text{m}} \times 10 \times 10^3 \text{ m} = 288 \text{ ns}$$

The maximum transmission bitrate in terms of the pulse r.m.s. width is given by

$$B_{T \max} = \frac{0.25}{\sigma_{\text{pulse}}} \quad (5.27)$$

Therefore, for $\sigma_s = \sigma = 288$ ns, the maximum bitrate is 868 Kbit/s, which is not a useful value for most modern applications.

The key question now is whether the differential delay for a multimode fiber can be improved. The reason the differential delay between the axial mode and the extreme meridional mode is high is that the meridional mode has to reach the boundary between core and cladding before it is reflected back into the core. If the flight time of a meridional mode is reduced, then the differential delay will also be reduced. This can be achieved with the use of graded index fiber.

The basic concept here is to vary the refractive index from a maximum at the center of the core to a minimum at the core-cladding interface. The general equation for the variation of refractive index with radial distance is

$$n(r) = \begin{cases} n_1(1 - 2\Delta(r/a)^\alpha)^{1/2} & r < a \text{ core} \\ n_1(1 - 2\Delta)^{1/2} = n_2 & r \geq a \text{ cladding} \end{cases} \quad (5.28)$$

where Δ is the relative refractive index difference, r is the axial distance, and a is the profile parameter that gives the refractive index profile. For $a = \infty$ the representation corresponds to the step index profile. Figure 5.14 illustrates the fiber refractive index for various values of the profile parameter a . The step index profile is obtained by setting $a = \infty$.

The improvement in differential delay can be observed by considering the modes of a multimode fiber with the profile parameter a set to 2 (Figure 5.15). Two effects may be observed. First, the axial mode propagates through the section of the fiber core where the refractive index has its maximum value, which implies that the axial mode is slowed down. The meridional modes are bent toward the axis of the fiber, reducing their flight time. Together these two effects reduce the differential delay.

If electromagnetic theory is employed to analyze the differential delay, the value obtained is

$$\Delta\tau_s|_{\text{graded}} = \frac{n_1 L}{c} \times \frac{\Delta^2}{8} = \Delta\tau_s|_{\text{step}} \times \frac{\Delta}{8} \quad (5.29)$$

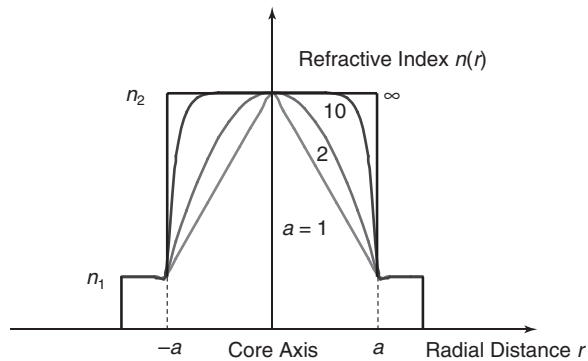


Fig. 5.14 Fiber refractive index for different values of the profile parameter a .

Source: Adapted from Senior (1992). Used with permission.

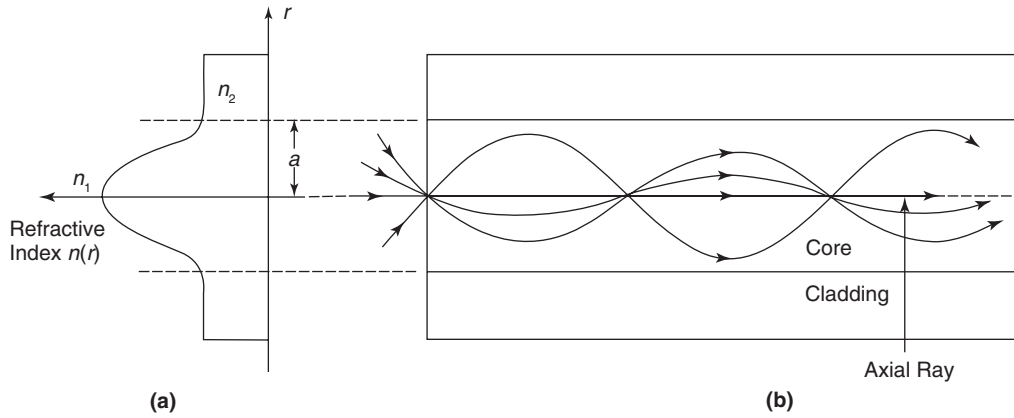


Fig. 5.15 Graded index multimode fiber: (a) refractive index profile; (b) meridional modes within the fiber. *Source:* Adapted from Senior (1992). Used with permission.

The implication of this equation is to highlight the fact that the reduction of the differential delay for step index fiber is $\Delta/8$. The r.m.s. pulse broadening is now given by

$$\sigma_{s|\text{index}} = \frac{n_1 L \Delta}{2 \times \sqrt{3} \times c} \times \frac{\Delta}{10} = \sigma_{s|\text{step}} \times \frac{\Delta}{10} \quad (5.30)$$

and there is a $\Delta/10$ reduction in the r.m.s. pulse broadening. It is now straightforward to compare the r.m.s. pulse broadening for step and graded index fibers. From the example studied before, we have a 10-km graded index fiber with a core refractive index of 1.5 and $\Delta = 2\%$. Then, from equation 5.30, the r.m.s. pulse broadening is

$$\sigma_{s|\text{index}} = \frac{n_1 L \Delta}{2 \times \sqrt{3} \times c} \times \frac{\Delta}{10} = \sigma_{s|\text{step}} \times \frac{\Delta}{10} = 288 \text{ ns} \times \frac{0.02}{10} = 0.576 \text{ ns}$$

and the maximum bitrate that can be used with this graded index fiber is now 434 Mbit/s!

Comparing the r.m.s. pulse broadening of the two fibers for a length of 1 km, one obtains

$$\sigma_{s|\text{step}} = 28.8 \text{ ns/km} \quad \text{and} \quad \sigma_{s|\text{graded}} = 0.057 \text{ ns/km}$$

Because of its substantially improved performance, graded index multimode fiber is the clear choice when one wants to exploit the advantages of the multimode fiber with low intermodal dispersion.

Multimode fibers have been fabricated in various core-cladding dimensions addressing specific requirements. For communication purposes two core-cladding sizes have been standardized.

The two fibers differ in the core size, with the first being $50 \mu\text{m}$ (ITU-I G standard G.651) and the second being $62.5 \mu\text{m}$. The cladding for both fibers is $125 \mu\text{m}$. At the moment

there are no standards for the 62.5- μm fiber. The major advantage of the 50/125 μm fiber is the higher bandwidth it offers compared to that of 62.5/125 μm at 850 nm. An advantage of the 62.5/125 μm is that more power can be coupled into the fiber from an optical device such as a Light Emitting Diode (LED) or laser because of the larger NA (NA = 0.275).

One of the important questions related to the performance of a fiber is that of the bandwidth. In general time and frequency domain techniques can be used to establish the performance, but the industry decided to adopt the bandwidth \times length product as the performance index of a multimode-fiber bandwidth.

A simple equation relating the bandwidth, BW , and the length of the fiber is

$$\frac{BW_L}{BW_S} = \left[\frac{L_L}{L_S} \right]^\gamma \quad (5.31)$$

where the subscripts L and S correspond to the bandwidth and length for long and short lengths of fiber, and the exponent γ is the length ratio of interest. Usually $\gamma = 1$, but there has long been debate about the value of γ because it reflects the conditions under which the measurements are taken. The value is calculated from the solution of equation 5.31—that is,

$$\gamma = \frac{\log \left[\frac{BW_L}{BW_S} \right]}{\log \left[\frac{L_L}{L_S} \right]} \quad (5.32)$$

In the rest of this section the value of $\gamma = 1$ will be assumed. The first-order estimate of the system length that a fiber can support is calculated from the given bandwidth \times length product. For example, for a bandwidth \times length product of 1000 MHz \times km the system length for a 2.4 Gbit/s system is

$$\text{System length} = \frac{\text{Bandwidth} \times \text{Length}}{\text{Bitrate}} = \frac{1000 \text{ MHz} \times \text{km}}{2.4 \times 10^3 \text{ MHz}} = 401 \text{ m}$$

When this approach is used to estimate the system length, one should understand the technique or techniques used to estimate the bandwidth \times length product of the fiber.

Some of the key parameters of the Corning InfiniCor graded index fiber (see Figure 5.11 for losses) are summarized in Tables 5.1 and 5.2. Similar fibers are available from other manufacturers.

The multimode fiber was introduced and discussed up to now with the tacit assumption that there are a large number of modes, but their number was not stated. This question will be addressed now. To derive the number of modes supported by a given multimode fiber,

Table 5.1 Attenuation of Corning InfiniCor Fiber

<i>Wavelength (nm)</i>	<i>Maximum value (dB/km)</i>
850	≤ 2.3
1300	≤ 0.6

Source: Corning Inc. Data Sheet, January 2008 Issue.

Table 5.2 Bandwidth \times km Performance of Corning InfiniCor Fiber

Corning Optical Fiber	High-performance 850 nm only (MHz \times km)	Legacy performance (MHz \times km)	
InfiniCor® eSX+	4700	1500	500
InfiniCor® SX+	2000	1550	500
InfiniCor® SXi	850	700	500
InfiniCor® 600	510	500	500

Source: Corning Inc. Data Sheet, January 2008 Issue.

the Maxwell equations must be solved in the context of the fiber structure (cylinder) and the material (dielectric, glass).

From such an analysis a very useful quantity emerges called normalized frequency, V . It combines the wavelength, the physical dimensions of the fiber, and the properties of the dielectric (glass), and is given by

$$V = \frac{2\pi}{\lambda} a \cdot (\text{NA}) = \frac{2\pi}{\lambda} \cdot a \cdot n_1(2\Delta)^{1/2} \quad (5.33)$$

where a is the core radius, Δ is the relative refractive index difference, and λ is the wavelength.

It can be shown that the number of modes supported by a step index multimode fiber, M_{step} , is

$$M_{\text{step}} \approx \frac{V^2}{2} \quad (5.34)$$

and by a graded index multimode fiber

$$M_{\text{graded}} \approx \left(\frac{\alpha}{\alpha + 2} \right) \cdot \left(\frac{V^2}{2} \right) \quad (5.35)$$

where α is the refractive index profile parameter. For a parabolic profile ($\alpha = 2$) the number of modes is $M_{\text{graded}} \approx V^2/4 = M_{\text{step}}/2$. Consider a multimode fiber operating at 1300 nm with radius 25 μm , $n_1 = 1.5$, and $\Delta = 2\%$. Then the step index fiber supports

$$V \approx \frac{2\pi}{\lambda} \cdot a \cdot n_1(2\Delta)^{1/2} = \frac{2 \times \pi}{1300 \times 10^{-9}} \times 25 \times 10^{-6} \times (2 \times 0.02)^{1/2} = 24$$

and

$$M_{\text{step}} \approx \frac{V^2}{2} = \frac{(24^2)}{2} = 288 \quad \text{guided modes}$$

With a parabolic refractive index profile the same fiber will support 156 guided modes. The number of modes and their fluctuations can impair the performance of a multimode fiber system because of modal noise.

After a pulse propagates in a fiber the r.m.s. pulse broadening s given by

$$\sigma_{\text{total}} = (\sigma_{\text{mat}}^2 + \sigma_{\text{w}}^2 + \sigma_{\text{mod}}^2)^{1/2} \quad (5.36)$$

where σ_{mat} is the material (chromatic) dispersion, σ_{w} is the waveguide dispersion (discussed in the next section), and σ_{mod} is the intermodal dispersion (for step index or graded index

fiber). For multimode transmission the material and waveguide dispersion terms are negligible compared to the intermodal dispersion, and they are usually ignored. Therefore, the pulse in the output of the fiber has an r.m.s. width given by

$$\sigma_{\text{out}} = (\sigma_{\text{inp}}^2 + \sigma_{\text{mod}}^2)^{1/2} \quad (5.37)$$

where σ_{inp} is the r.m.s. width of the input pulse.

Single-Mode Fibers

In the section The Structure and Physics of an Optical Fiber, the concept of the single-mode fiber was introduced, and the most important physical feature of a single-mode fiber is its small core. For a useful image of how a single-mode fiber operates, one can use the idea that only the axial mode propagates in the fiber. The bandwidth of single-mode fiber is so large compared to that of the multimode fiber that single-mode fiber is used in all long-haul communications today, terrestrial and submarine. Concepts used to arrive at a reasonable understanding of the propagation features of multimode fiber cannot be used in single-mode fibers, and the solution of Maxwell equations in the context of the geometry and materials is required. Only the results of the mathematical analysis based on Maxwell equations will be presented in this section.

The spectral loss of a single-mode fiber is that shown in Figure 5.8. This is a research result, but we will see that single-mode fibers are available with these loss characteristics as products for terrestrial and submarine applications.

The most striking difference between multimode and single-mode fibers is in the dispersion. In multimode fibers the total dispersion is dominated by the intermodal dispersion. In single-mode fibers only one propagation mode is supported, so the total dispersion consists of three components: material dispersion, waveguide dispersion, and polarization mode dispersion.

The reason waveguide dispersion and polarization mode dispersion became important is the low value of the material dispersion. The normalized frequency parameter, V , plays an important role in single-mode fiber. The parameter V is given by

$$V = \frac{2\pi a}{\lambda} \cdot n_1(2\Delta)^{1/2} \quad (5.38)$$

where the symbols have their usual meaning. Single-mode operation takes place above a theoretical cutoff wavelength λ_c given from equation 5.38 as

$$\lambda_c = \frac{2\pi a}{V_c} \cdot n_1(2\Delta)^{1/2} \quad (5.39)$$

where V_c is the cutoff normalized frequency. With the help of equation 5.38, equation 5.39 can be written as

$$\frac{\lambda_c}{\lambda} = \frac{V}{V_c} \quad (5.40)$$

For a step index single-mode fiber—that is,

$$n(r) = \begin{cases} n_1 & r < a \quad \text{core} \\ n_2 & r \geq a \quad \text{cladding} \end{cases} \quad (5.41)$$

$V_c = 2.405$ and the cutoff wavelength is given by

$$\lambda_c = \frac{V\lambda}{2.405} \quad (5.42)$$

For operation at 1300 nm the recommended cutoff wavelength ranges from 1100 to 1280 nm. With this choice for the cutoff wavelength, operation at 1300 nm is free of modal noise and intermodal dispersion. The material dispersion for silica glass with a step index single-mode fiber is given by

$$D_m(\lambda) \approx \frac{\lambda}{c} \cdot \frac{d^2 n_1}{d^2 \lambda} \quad (5.43)$$

where $d^2 n_1 / d^2 \lambda$ is the second derivative of the refractive index with respect to the wavelength.

The value of $D_m(\lambda)$ is usually estimated from fiber measurements, but for theoretical work a simple equation with two parameters offers a reasonable approximation. The equation is

$$D_m(\lambda) = \frac{S_0 \lambda}{4} \cdot \left[1 - \left(\frac{\lambda_0}{\lambda} \right)^4 \right] \quad (5.44)$$

where S_0 and λ_0 are the slope at λ_0 and the zero material dispersion wavelength, respectively. For standard single-mode fiber the slope at λ_0 is in the range 0.085 to 0.095 ps/nm² × km.

The Corning single-mode fiber SMF-28e+ is a typical example of high-quality modern fiber whose key parameters are summarized next. For this Corning fiber, equation 5.44 is valid for the range $1200 \leq \lambda \leq 1625$ nm. Tables 5.3, 5.4, and 5.5 summarize the performance of the Corning SMF-28e+ fiber. Single-mode fibers of similar performance are also available from other fiber manufacturers.

After material dispersion the next important dispersion component is waveguide dispersion. The physical origin of waveguide dispersion is the wave-guiding effects, and even without material dispersion, this term is present. A typical waveguide dispersion curve is shown in Figure 5.16.

The importance of this term is not so much in the value of the dispersion but in the sign. In silica fiber the waveguide dispersion is negative, and because the material disper-

Table 5.3 Attenuation of Corning SMF-28e+™ Single-Mode Fiber

Wavelength (nm)	Maximum values (dB/km)
1310	0.33–0.35
1383	0.31–0.33
1490	0.21–0.24
1550	0.19–0.20
1625	0.20–0.23

Source: Corning Inc. Data Sheet, December 2007 Issue.

Table 5.4 Single-Mode Fiber Dispersion of Corning SMFe+ in the Third Optical Window

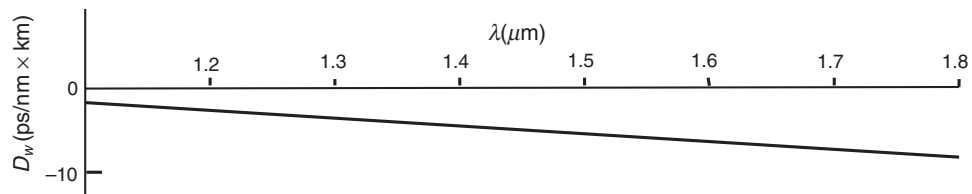
Wavelength (nm)	Dispersion value [ps/(nm × km)]
1550	≤18.0
1625	≤22.0

Source: Corning Inc. Data Sheet, December 2007 Issue.

Table 5.5 Zero-Dispersion Wavelength and Slope of Corning SMF-28e+ Single-Mode Fiber

Zero-dispersion wavelength (nm)	$1310 \leq \lambda_0 \leq 1324$
Zero-dispersion slope [ps/(nm ² × km)]	$S_0 \leq 0.092$
λ_0 typical value (nm)	1317
S_0 typical value [ps/(nm ² × km)]	0.088

Source: Corning Inc. Data Sheet, December 2007 Issue.

**Fig. 5.16** Waveguide dispersion with $\lambda_c = 1.2$ and $\Delta = 0.003$.

sion is positive above λ_0 , the value of the total dispersion is reduced. The immediate impact is to shift λ_0 to longer wavelengths. By itself this small shift in λ_0 is of marginal importance, but if the value of the waveguide dispersion is designed to take much higher values, then the shift is substantial and gives rise to two new classes of single-mode fiber: dispersion shifted and dispersion flattened, which will be discussed in the next section.

The third component of dispersion in single-mode fiber is polarization mode dispersion, or PMD. For ease of study it has been assumed tacitly that the fiber is a perfect cylindrical structure. In reality the structure is only nominally cylindrical around the core axis. The core can be slightly elliptical. Also, the cabling process can impose strain on the fiber, or the fiber might be bent as it is installed.

In these situations the fiber supports the propagation of two nearly degenerative modes with orthogonal polarizations. When the optical wave is modulated by the carried information, the two waves corresponding to the two states of polarization are modulated. Therefore, two modes orthogonal to each other propagate in the waveguide. In systems where the receiver can detect both states of polarization, the receiver will function as expected if both modes arrive at the same time; that is, there is no differential delay between the two modes. However, the refractive index of the silica glass can be slightly different along the two orthogonal axes, and consequently there is differential delay. The average Differential Group Delay (DGD) is the PMD coefficient of the fiber.

$$\text{PMD} = \langle \text{DGD} \rangle \tag{5.45}$$

To compound the difficulties, the DGD is not the same along the length of the fiber but varies from section to section. Because of this feature, the PMD is not described by a single value but rather by a probability distribution function. The impact of PMD on pulse width is illustrated in Figure 5.17.

The PMD is a complex effect, and its study and mitigation have attracted a very substantial effort. Theoretical studies and experiments have demonstrated that the PMD is proportional to the square root of the fiber length—that is,

$$D_{\text{PMD}} = \text{PMD}_{\text{coeff}} \sqrt{L} \quad \text{ps}\sqrt{\text{km}} \tag{5.46}$$

Because of its importance for high-speed systems, the PMD fiber coefficient is part of the fiber specifications. For example, the Corning fiber STM-28e+ has a PMD coefficient of $\leq 0.06 \text{ ps}/\sqrt{\text{km}}$.

The calculation of the amount of PMD a system can tolerate is an involved process and is part of the system design. An easily remembered guideline is that the PMD of the link satisfies the inequality

$$D_{\text{PMD}} \leq \frac{\text{Pulse width}}{10} \tag{5.47}$$

The impact of PMD on high-speed systems is quite severe, as can be seen from Table 5.6. From this table it is clear that long-haul high-capacity systems are very vulnerable to PMD, and the selection of the fiber type is a very important decision in system design.

The ITU-T has issued standards for the conventional fiber that are described by the G.652 recommendation. The fiber covered by this recommendation is the most widely installed in the worldwide telecommunications network.

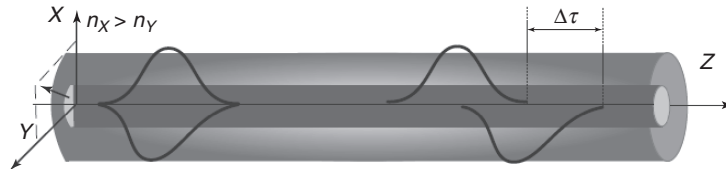


Fig. 5.17 Effect of PMD on a pulse. Source: Corning Inc.

Table 5.6 Impact of PMD on System Length for Typical Bitrates

Bitrate (Gbit/s)	Timeslot (ps)	Link PMD (ps)	System length (km)	
			$\text{PMD}_{\text{coeff}} 0.02 \text{ ps}/\sqrt{\text{km}}$	$\text{PMD}_{\text{coeff}} 0.5 \text{ ps}/\sqrt{\text{km}}$
2.5	400	40.0	4.0×10^6	6.4×10^3
10.0	100	10.0	2.5×10^5	4.0×10^2
40.0	25	2.5	15.6×10^3	25.0
100.0	10	1.0	2.5×10^3	4.0

Until now the discussion has been limited to what may be called the conventional single-mode fiber. That is a single-mode fiber with $\lambda_0 \approx 1300$ nm, low waveguide dispersion ($D_m \geq D_w$), and a step index profile. Since the introduction of the conventional single-mode fiber, a number of applications have arisen where a fiber optimized for the application can deliver better performance. We are now going to take a very brief look at these special fibers.

Special Single-Mode Fibers

As was mentioned in the Single-Mode Fibers section, waveguide dispersion can be used to shift the λ_0 of a fiber to a direction that the dispersion of the fiber will be substantially altered. Initially, two classes of fiber emerged to exploit this property of waveguide dispersion. The first was the dispersion-shifted fiber in which the value of the waveguide dispersion was large and the λ_0 shifted to 1550 nm. At this wavelength the zero dispersion and the minimum loss value of silica glass coincided, offering the best of both worlds: dispersion and loss. This fiber design favors Electrical Time Division Multiplexed (ETDM) systems, and it was introduced at a time when the only practical way to increase the capacity appeared to be ETDM.

Later, however, a better approach in terms of cost-performance was identified with Wavelength Division Multiplexing (WDM), and another fiber was introduced in which the dispersion presented a plateau enabling the WDM channels to face similar dispersion. Unfortunately, again the fiber could not be employed in large quantities because of the nonlinear behavior of the silica fiber when optical amplifiers are used (see the section on nonlinear fiber effects) demands the presence of substantial dispersion between channels if the nonlinear effects are to be mitigated. Therefore, the two first attempts to break the confines of the conventional single-mode fiber were not very successful. The dispersion characteristics of standard fiber, dispersion-shifted fiber, and dispersion-flattened fiber are shown in Figure 5.18.

The dispersion-shifted fiber standards are addressed in ITU-T recommendation G.653.

The introduction of the erbium-doped silica optical amplifier operating over the band 1530 to 1565 nm and the suppression of the OH loss peak prompted the division of the

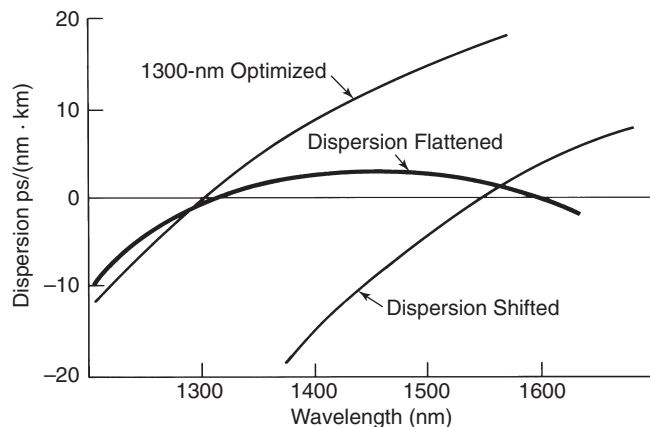


Fig. 5.18 Dispersion characteristics of standard, dispersion-flattened, and dispersion-shifted fibers.

Source: Adapted from Senior (1992). Used with permission.

Table 5.7 Optical Bands Available for Fiber Communications with SiO₂ Fibers

<i>Band</i>	<i>Description</i>	<i>Wavelength range</i>
O-band	Original band	1260–1360 nm
E-band	Extended band	1360–1460 nm
S-band	Short-wavelengths band	1460–1530 nm
C-band	Conventional (erbium window)	1530–1565 nm
L-band	Long-wavelengths band	1565–1625 nm
U-band	Ultralong-wavelengths band	1625–1675 nm

Table 5.8 Attenuation of Nonzero Dispersion-Shifted Fiber

<i>Wavelength (nm)</i>	<i>Loss (dB/km) Maximum</i>	<i>Loss (dB/km) Typical</i>	The maximum attenuation in the range 1525–1625 nm is no more than 0.05 dB/km greater than the attenuation at 1550 nm.
1310 nm	≤0.40	≤0.35	
1383 nm	≤0.40	≤0.25	
1450 nm	<0.26	≤0.25	
1550 nm	≤0.22	≤0.20	
1625 nm	≤0.24	≤0.21	

Source: Copyright © 2005 Furukawa Electric North America, Inc.

Table 5.9 Dispersion of Nonzero Dispersion-Shifted Fiber

<i>Optical band</i>	<i>Dispersion ps/(nm × km)</i>	Zero dispersion wavelength: ≤1405 nm Dispersion slope at 1550 nm: ≤0.045 ps/nm ² ·km Mode field diameter: 8.6 ± 0.4 μm at 1550 nm
C-band 1530–1565 nm	5.5–8.9 ps/nm·km	
L-band 1565–1625 nm	6.9–11.4 ps/nm·km	
S- and L-bands 1460–1625 nm	2.0–11.4 ps/nm·km	

Source: Copyright © 2005 Furukawa Electric North America, Inc.

available low loss window of the silica fiber into a number of bands whose exploitation will depend on the availability of the relevant technology. A summary of the optical bands and their respective wavelengths is summarized in Table 5.7.

A number of fibers have been introduced to address the use of these optical bands. The aim is to reduce the amount of dispersion in the intended band of operation and also to minimize the impact of fiber nonlinearities. According to the ITU-T G.655 recommendations, the dispersion over the C-band should lie in the range 1 to 10 ps/(nm × km). Then the operation can be extended into the L-band because the dispersion will still be low there. Both C- and L-bands are used for long haul applications. ITU-T recommendation G.656 is designed to extend operation into the S-band. With chromatic dispersion in the range of 2 to 14 ps/(nm × km) from 1460 to 1625 nm, this fiber can be used for Coarse WDM (CWDM) and Dense WDM (DWDM) throughout the S-, C-, and L-bands. These fibers are referred to as Non-Zero Dispersion-Shifted Fibers (NZ-DSF).

A summary of the performance of the Furukawa Electric North America, Inc., NZ-DSF fiber is given in Tables 5.8 and 5.9.

The dispersion of the NZ-DSF at 1550 nm is nearly four times less than that of the standard single-mode fiber, reducing the amount of dispersion compensation needed in

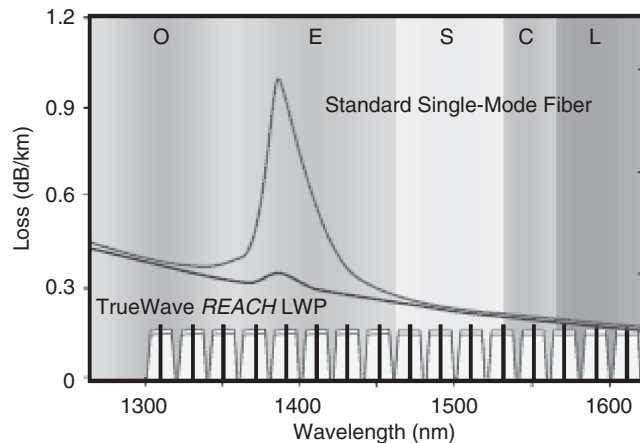


Fig. 5.19 Use of NZ-DSF in a coarse WDM channel allocation scheme.

Source: Copyright © Furukawa Electric North America, Inc.

long-haul systems (see Chapter 6). The reader should be aware that all leading fiber manufacturers market NZ-DSF fiber.

A significant part of the cost of DWDM systems is the cost of the narrowband active and passive optical components required by the specifications. The availability of the NZ-DSF fibers has enabled a substantial reduction of the cost of WDM by spacing the channels at 20 nm. This channel spacing accommodates 16 channels from 1310 to 1625 nm and is supported by ITU-T recommendation G.652C. A schematic of the spectral loss and the CWDM channel scheme is shown in Figure 5.19.

Special Fibers

The discussion so far has been limited to fibers designed for transmission. However, there are a large number of fibers designed with the aim of addressing special requirements. By virtue of necessity we will outline briefly the fibers designed for special needs in the field of optical communications.

Erbium-doped silica fiber. This fiber is used as the gain medium in optical fiber amplifiers for the C-band of the spectrum (1530–1565 nm).

Polarization-preserving fiber. This fiber is used in situations where the polarization of the optical radiation inhibits the use of nonpolarization preserving fibers. Bearing in mind that the normal transmission fiber does not preserve polarization, polarization-preserving fibers are used in laser fiber tails, external modulators, polarization mode dispersion compensators, and in general devices (active and passive) that require control of the polarization of the radiation.

Photosensitive fiber. This fiber is used in the fabrication of Bragg gratings, which are used in dispersion compensators employing the Bragg effect and other optical fiber components.

Bend-insensitive fiber. The aim of this fiber is to minimize the losses due to the tight bending of fibers and finds applications in the packaging of optical devices.

The parameters of the fibers previously enumerated vary from manufacturer to manufacturer, and the reader is encouraged to look at the Web sites of fiber manufacturers.

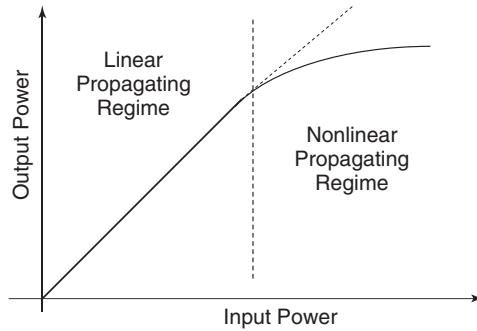


Fig. 5.20 Typical nonlinear characteristic of optical fiber.

Nonlinear Optical Effects in Fibers

The discussion of fiber performance was based implicitly on a linear model. That is, when the input is doubled the output is also doubled. However, the optical fiber is essentially a waveguide loaded with a dielectric material, the glass, and under suitable conditions the behavior of the glass departs from a linear characteristic. This is illustrated in Figure 5.20, where the input to output relationship is no longer linear.

The study of nonlinear optical effects belongs to the field of nonlinear optics, but because the effects on optical fiber communications are serious, a brief outline will be presented here (see also Chraplyvy et al., 1984).

The origin of nonlinear optical effects lies in the response of the atoms and molecules of the glass dielectric in high electric fields. One might be surprised that in spite of the low optical powers used in fiber communications, the nonlinear behavior of the fiber impairs system performance.

The electric field in a medium with effective area A_{eff} and power P is given by

$$|E| = \sqrt{\frac{2 \times 377}{n}} \times \sqrt{\frac{P}{A_{\text{eff}}}} \quad (5.48)$$

With a semiconductor laser of 10 mW and a fiber with an effective area of $53 \mu\text{m}^2$, the electric field in the fiber is

$$|E| = \sqrt{\frac{2 \times 377}{n}} \times \sqrt{\frac{P}{A_{\text{eff}}}} = \sqrt{\frac{2 \times 377}{1.5}} \times \sqrt{\frac{10 \times 10^{-3}}{53 \times 10^{-12}}} = 3.0 \times 10^5 \text{ V/m}$$

The electric field experienced by the electron in the hydrogen atom is of the order of $5 \times 10^{11} \text{ V/m}$, so one could think that the field generated by a laser beam of 10 mW would not give rise to nonlinear optical effects. Although the optical power is low, the interaction length between the optical radiation and the glass dielectric can be very long when the fiber operates with optical amplifiers. The effect is cumulative, and system performance is impaired.

The channel power used in this simple example refers to one laser, but in a WDM system the number of channels can exceed 100, so the total power can be very high.

In nonlinear effects associated with the propagation of light in fibers there are two fiber parameters that dimension the impact of the effects. The first is the effective area of the radiation mode, A_{eff} . It is defined as shown in equation 5.51:

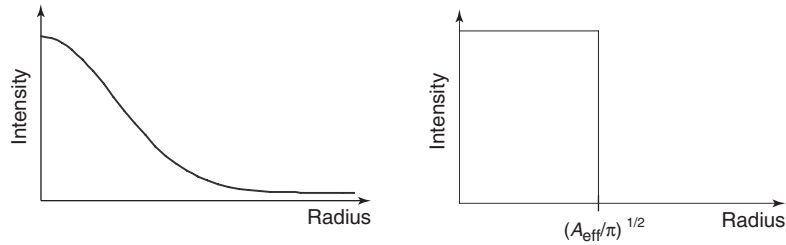


Fig. 5.21 Concept of the effective area of A_{eff} .

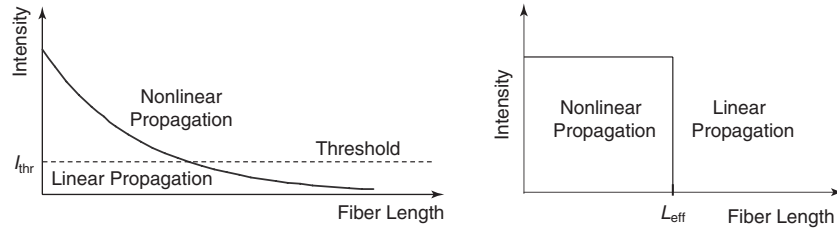


Fig. 5.22 Concept of the effective length, L_{eff} , in nonlinear optical effects.

$$A_{\text{eff}} = \pi r_0^2 \quad (5.49)$$

where r_0 is the mode field radius. The concept is illustrated in Figure 5.21.

The second is the effective length, L_{eff} , and it is defined by

$$L_{\text{eff}} \equiv \int_0^L \exp(-\alpha z) dz = \frac{1 - \exp(-\alpha L)}{\alpha} \quad (5.50)$$

where L is the fiber length and α is the attenuation coefficient of the fiber, which here is not in dBs. The attenuation coefficient of the fiber in this equation is derived from the loss in decibels through the equation

$$\alpha = \frac{\alpha_{\text{dB}}}{4.343} \quad (5.51)$$

For low-loss fiber $L_{\text{eff}} \approx L$ and for high loss fiber, $L_{\text{eff}} \approx 1/\alpha$. Because the fiber for optical transmission has low loss, the first approximation is usually used. The physical meaning of L_{eff} is simple. We know that for low power the nonlinear effects are negligible, so there is a "threshold" of power above which the propagation is nonlinear and below which it is linear. This concept is illustrated in Figure 5.22.

For example, consider a fiber with a loss of 1.8 dB/km and length of 25 km. Using the approximation for low loss, $L_{\text{eff}} \approx L$. If we use equation 5.50 the result is 15.5 km. In a system with optical amplifiers, the effective length of the system is given by

$$L_{\text{eff}} = \frac{1 - \exp(-\alpha l)}{\alpha} \times \frac{L_{\text{total}}}{\Delta l} \quad (5.52)$$

where L_{total} is now the total system length and Δl the spacing between amplifiers. It is clear that to reduce the system effective length it is better to use as few amplifiers as possible.

The nonlinear effects relevant to fiber communications are

- [1] Single-channel systems
 - [1a] Self-Phase Modulation (SPM)
 - [1b] Stimulated Brillouin Scattering (SBS)
- [2] Multichannel systems
 - [2a] Cross-Phase Modulation (XPM)
 - [2b] Stimulated Raman Scattering (SRS)
 - [2c] Four-Wave Mixing (FWM)

[1a] Self-Phase Modulation

To understand the self-phase modulation effect, one has to understand the effect of high intensity on the refractive index of the material. This impact of optical power on the refractive index can be stated mathematically as

$$n(t) = n_1 + \Delta n(t) = n_1 + n_2 E^2(t) \quad (5.53)$$

where n_1 is the conventional refractive index of the silica glass and n_2 is the nonlinear refractive index. The value of n_2 is $3.2 \times 10^{-20} \text{ m}^2/\text{W}$ and it is therefore very small compared to the linear refractive index, n_1 , which for silica glass at 1550 nm is 1.444. The difference is 20 orders of magnitude, but the impact of n_2 is still important because of the long length interaction between material and radiation and the high intensity of the radiation.

Over a fiber length L the total phase shift due to $\Delta n(t)$ is given by

$$\Delta\phi(t) = \int_0^L \frac{\omega_0}{c} \Delta n(t) dz = \int_0^L \frac{2\pi}{\lambda} \Delta n(t) dz = \frac{\omega_0}{c} n_2 E^2(t) L \quad (5.54)$$

$$\Delta\omega(t) = -\frac{d}{dt} \Delta\phi(t) = -\frac{d}{dt} \left[\frac{\omega_0}{c} n_2 E^2(t) \right] L \quad (5.55)$$

To proceed, one needs an analytical expression of the electric field. For convenience let us assume that the input light pulse has a Gaussian envelope:

$$E(t) = E_0 \exp \left[-\frac{(t-t_0)^2}{\tau^2} \right] \quad (5.56)$$

where E_0 is the peak pulse amplitude, t_0 is the time position of the pulse, and τ is the half-width at the $1/e$ point of the peak amplitude. Substituting equation 5.56 into equation 5.54, we obtain

$$\Delta\phi(t) = \Delta\phi_{\text{max}} \exp \left[-\frac{2(t-t_0)^2}{\tau^2} \right] \quad (5.57)$$

$$\Delta\phi_{\text{max}} = \frac{\omega_0}{c} n_2 E_0^2 L \quad (5.58)$$

where the length L corresponds to the nonlinear interaction length, L_{eff} . The maximum frequency change is obtained by substituting equation 5.57 into equation 5.55:

$$\Delta\omega(t) = \Delta\phi_{\text{max}} \frac{4(t-t_0)}{\tau^2} \exp\left[-\frac{2(t-t_0)^2}{\tau^2}\right] \quad (5.59)$$

At the center of the pulse the frequency shift is zero. To find the position of the maximum frequency shift we calculate

$$\frac{d}{dt}[\Delta\omega(t)=0] \quad (5.60)$$

One finds that the maximum frequency changes occur at $(t - t_0) = \pm\tau/2$. For example, consider the Gaussian pulse with $\tau = 1$ psec, $\Delta\phi_{\text{max}} = 8\pi$. The results are summarized in Figure 5.23.

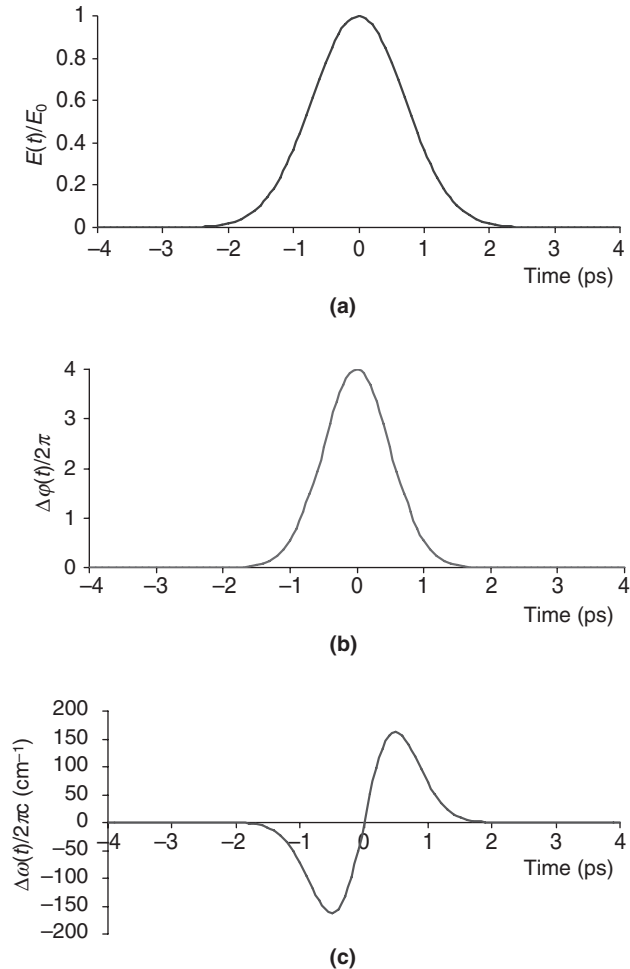


Fig. 5.23 (a) Normalized input pulse amplitude; (b) phase shift due to nonlinearity; (c) frequency chirp.



Fig. 5.24 SPM followed by negative and positive dispersion: (a) $D < 0$, additional pulse broadening; (b) $D > 0$, pulse compression.

For the central position of the pulse the frequency chirp is linear between $\pm\tau/2$ and is given by

$$\omega(t) = \omega_0 + \left(\frac{4\pi n_2}{\lambda_0 \tau^2} L \frac{P}{A_{\text{eff}}} \right) \times t \quad (5.61)$$

The impact of SPM on the performance of an optical system depends on the dispersion. If there were no dispersion in the fiber, SPM would have no impact on performance.

First consider operation at $\lambda > \lambda_0$. Then $D < 0$ and the pulse will broaden because the leading “red” frequencies travel faster and the “blue” frequencies slower. For $\lambda > \lambda_0$ the situation changes substantially. Now, the “red” frequencies in the rising edge of the pulse are delayed and the “blue” frequencies at the falling edge are speeded up; consequently, the pulse width contracts. However, as the blue frequencies catch up with the red ones and overtake them, the pulse starts broadening again.

This feature of the interaction of SPM with anomalous dispersion is used in soliton transmission. Figure 5.24 summarizes the interaction of SPM with fiber dispersion.

[1b] Stimulated Brillouin Scattering

The physical origin of Stimulated Brillouin Scattering (SBS) is the interaction between an incident optical wave and the elastic acoustic wave induced by the radiation. A threshold can be established for the onset of SBS, and it is given by

$$P_{\text{th}}^{\text{Brillouin}} \approx 21 \times p_{\text{Pol}} \times \frac{A_{\text{eff}}}{g_{\text{B}} L_{\text{eff}}} \times \left(1 + \frac{\Delta f_{\text{source}}}{\Delta f_{\text{Br}}} \right) \quad (5.62)$$

where p_{Pol} takes the value 1.5 if the polarization is completely scrambled and 1.0 otherwise; A_{eff} is the effective area of the mode; g_{B} is the Brillouin (Br) gain, which is around 4×10^{-11} m/W at 1550 nm; L_{eff} is the effective fiber length; Δf_{source} is the bandwidth of the incident radiation; and Δf_{Br} is the bandwidth of the SBS effect, which is approximately 20 MHz.

In the worst case for $\Delta f_{\text{source}} \ll \Delta f_{\text{Br}}$ and $p_{\text{Pol}} = 1$ with $A_{\text{eff}} = 50 \mu\text{m}^2$ and $L_{\text{eff}} = 20$ km the threshold power is 1.3 mW. This is very low and care must be taken to enhance the threshold. For high-speed modulation this is not a problem. In SBS the scattered wave propagates backward and the effect appears in the receiver as a reduction of the power of the wave carrying the information. Figure 5.25 illustrates the basic features of SBS.

The SBS is a narrowband effect and consequently does not interact with other waves unless they fall within its bandwidth. For this reason SBS once suppressed in individual channels is not an issue in WDM systems.

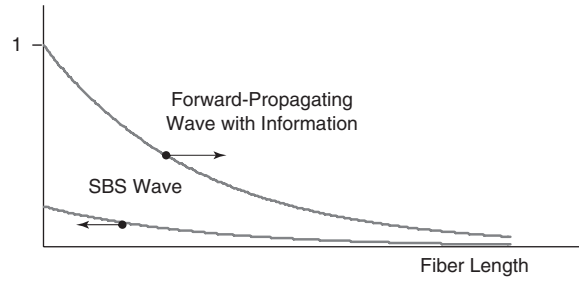


Fig. 5.25 Stimulated Brillouin scattering (SBS) effect.

[2a] Cross-Phase Modulation

The SPM discussed earlier operates within each channel. However, if a channel has enough power to induce the effect on the refractive index of the material for another channel propagating through the same material (that is to say, in a WDM system) then impairment arises in this other channel. This effect is referred to as Cross-Phase Modulation (XPM). The total induced frequency chirp, $\Delta\omega_{NL}(t)$, is given by

$$\Delta\omega_{NL}(t) = -\gamma \times L_{\text{eff}}^{\text{System}} \times \left(\frac{\partial P_n}{\partial t} + 2 \sum_{j \neq n}^N \frac{\partial P_j}{\partial t} \right) \quad (5.63)$$

where

$$\gamma = \frac{2\pi n_2}{\lambda A_{\text{eff}}} \quad (5.64)$$

Because the XPM term is twice that of a single channel in the first-order design of WDM, only the XPM term is taken into consideration.

[2b] Stimulated Raman Scattering

With an very intense incident optical wave, Stimulated Raman Scattering (SRS) can occur in which a forward-propagating wave, referred to as the Stokes wave, grows rapidly in the fiber so that most of the energy of the incident wave is transferred into it. The incident radiation is also referred to as the pump.

In a fiber the forward-scattered wave grows as

$$I_s(L) = I_s(0) \times \exp(g_R I_p L_{\text{eff}} - \alpha_S L) \quad (5.65)$$

where g_R is the Raman gain coefficient; I_p is the intensity of the incident radiation; $I_s(0)$ is the initial value of the forward-scattered wave; L_{eff} is the effective length; α_S is the fiber loss at the wavelength of the Stokes wave; and L is the fiber length. The Raman gain, g_R , in silica fiber extends over a large frequency range (up to 40 THz) with a broad peak near 13 THz.

This behavior is due to the noncrystalline nature of silica glass. In amorphous materials such as fused silica, molecular vibrational frequencies spread out into bands that overlap and become a continuum, unlike most materials where Raman gain occurs at specific frequencies. The Raman gain for silica is shown in Figure 5.26 measured with a pump at 1.0 μm .

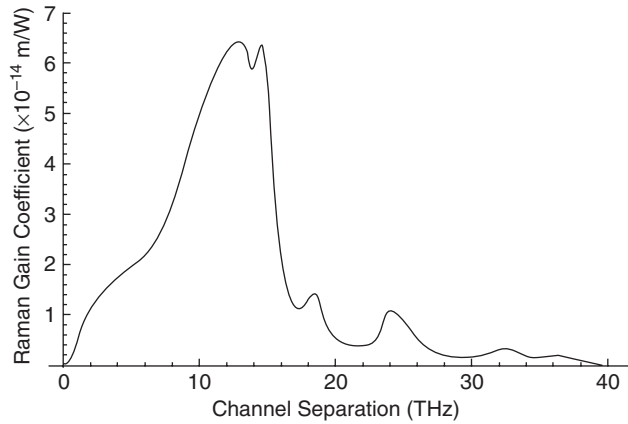


Fig. 5.26 Raman gain of silica fiber.

Source: Based on Ramaswami and Sivarajan (2002) and Stolen (1980).

The impact of the SRS on the performance of a single-channel optical system is negligible because the threshold power required is

$$P_{\text{th}}^{\text{Raman}} \approx 16 \frac{A_{\text{eff}}}{g_R L_{\text{eff}}} \quad (5.66)$$

and for a fiber with $A_{\text{eff}} = 50 \mu\text{m}^2$, $g_R = 6 \times 10^{-14} \text{ m/W}$ and with $L_{\text{eff}} = 20 \text{ km}$, the threshold is reached for 0.666 W.

Considering that optical systems are low-power systems in terms of optical power, single-channel systems are not affected by SBS. With optical amplifiers and single-channel systems one has to use equation 5.50 for L_{eff} . The threshold given by equation 5.66 is defined as the threshold at which the power of the forward-scattered wave, the Stokes wave, equals the incident radiation (pump).

The Raman gain coefficient at 1550 nm is approximately $6 \times 10^{-14} \text{ m/W}$. This is of course much smaller than the gain coefficient of SBS, but the fundamental difference is in the bandwidth of the two processes. From Figure 5.26 the gain extends up to 15 THz (125 nm), and two waves 125 nm apart will still be coupled. Although SRS is of no particular importance in the performance of single-channel systems, in WDM systems it becomes very important.

The reason for this is the wide bandwidth of the SRS. Let us consider a WDM system and one wavelength, say λ_0 , that is at 10 THz in the Raman gain profile. All the channels with shorter wavelengths act as pumps and amplify the wavelength at λ_0 , losing photons (power) in the process. The SRS process can be used for optical amplification, and the amplifiers using it are referred to as Raman amplifiers. In a WDM system the SRS can lead to performance impairments if care is not taken. Figure 5.27 illustrates the effect of SRS in a four-channel WDM system.

It is clear that SRS cannot be avoided in WDM systems, and the way to handle it is to accept impairment in system performance and design with this as a constraint. If this approach is acceptable, then the loss of power to the channel of the shortest wavelength is the constraint. After some assumptions, such as that (1) the channel spacing is equal, (2) the power in each channel is the same, and (3) all channels fall within the Raman gain

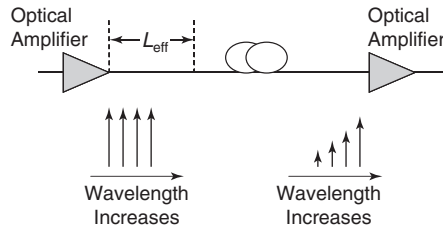


Fig. 5.27 Impacts of SRS in a four-channel WDM system. Notice that the channel of the shortest wavelength is most depleted.

bandwidth, the power loss by the channel with the shortest wavelength, say channel 0, is given by

$$P_0 = \frac{[(N-1)\Delta f][NP_{\text{ch}}]}{6 \times 10^4} \times \frac{g_{\text{Rpeak}} \times L_{\text{eff}}}{A_{\text{eff}}} = \frac{B_{\text{total}} \times P_{\text{total}}}{6 \times 10^4} \times \frac{g_{\text{Rpeak}} \times L_{\text{eff}}}{A_{\text{eff}}} \quad (5.67)$$

The penalty for channel 0 is now given by

$$\text{Penalty}|_0 = -10 \log[1 - P_0] \quad (5.68)$$

If a penalty equal to or less than 0.5 dB is desired, then $P_0 \leq 0.1$ and after some changes in the units of parameters,

$$P_{\text{total}} \times B_{\text{total}} \times L_{\text{eff}} < 40 \times 10^3 \text{ mW} \times \text{nm} \times \text{km} \quad (5.69)$$

This equation is conservative because it ignores chromatic dispersion; with chromatic dispersion in the system the right side of equation 5.69 is nearly doubled. Using a channel spacing of 0.8 nm (10 GHz), an amplifier spacing of 80 km, and an L_{eff} of 20 km, the limitations imposed on channel power by SRS are shown in Figure 5.28.

It is clear that for a small number of channels SRS does not impose a strong upper bound on power per channel, but for a large number of channels care should be taken to control the impact of SRS.

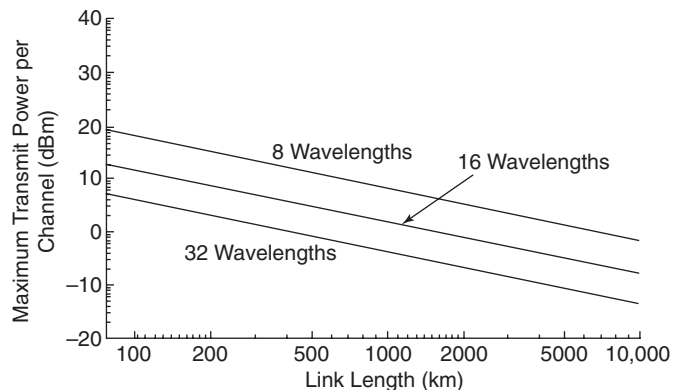


Fig. 5.28 Maximum power limitations imposed by SRS in a WDM system.

Source: Based on Ramaswami and Sivarajan (2002).

[2c] Four-Wave Mixing

The origin of four-wave mixing is the dependency of refractive index on optical power. This dependency not only gives rise to SPM but also induces new frequencies to appear. This effect is called Four-Wave Mixing (FWM) and it is independent of the bitrate but dependent on channel spacing and the chromatic dispersion present in the propagation path. It is a complex effect to analyze, but FWM efficiency is reduced by increasing the channel spacing and the chromatic dispersion between channels. New frequencies are generated by the process

$$\omega_{ijk} = \omega_i + \omega_j - \omega_k \quad \text{with } i, j \neq k \quad (5.70)$$

where the indices i , j , and k refer to the frequencies present. Assuming that N frequencies are present, the number of new frequencies is given by

$$\text{Number of new frequencies} = N(N-1)^2 \quad (5.71)$$

As an example, consider a three-channel system. The number of new frequencies expected to be induced by the process is 12. The spectrum of the 12 new frequencies is shown in Figure 5.29.

It is clear that the penalty of FWM is twofold: First, there is loss of power to the new frequencies generated but falling outside the bandwidth of the original three-channel system; second, there is interference as some of the new frequencies coincide with the original frequencies. The assessment of the performance is complex, and we can only illustrate the impact of performance for a few cases (see Figure 5.30).

It should be clear that the impact increases as the dispersion between channels decreases (for conventional single-mode fiber and dispersion-shifted fiber) and the channel spacing is reduced.

Closing this section on nonlinear fiber effects, one might wonder what fiber parameters one should expect from a fiber suitable for long-haul multichannel operation. The key to answering this question is equation 5.67. From that equation it is clear that the propensity of the fiber to induce nonlinear effects depends on the effective area. For this reason fiber manufacturers have introduced fibers with larger effective areas. For example, the Large

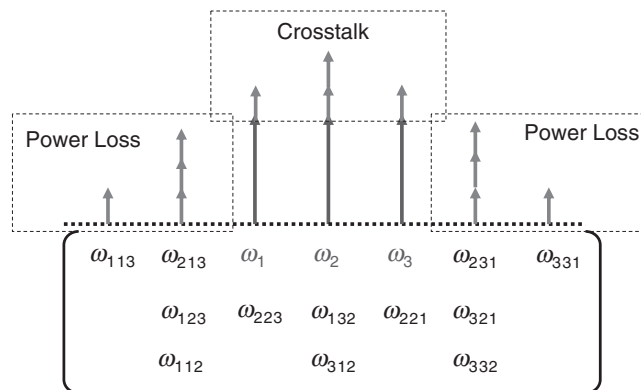


Fig. 5.29 Spectrum generated from a FWM process for a three-channel system.

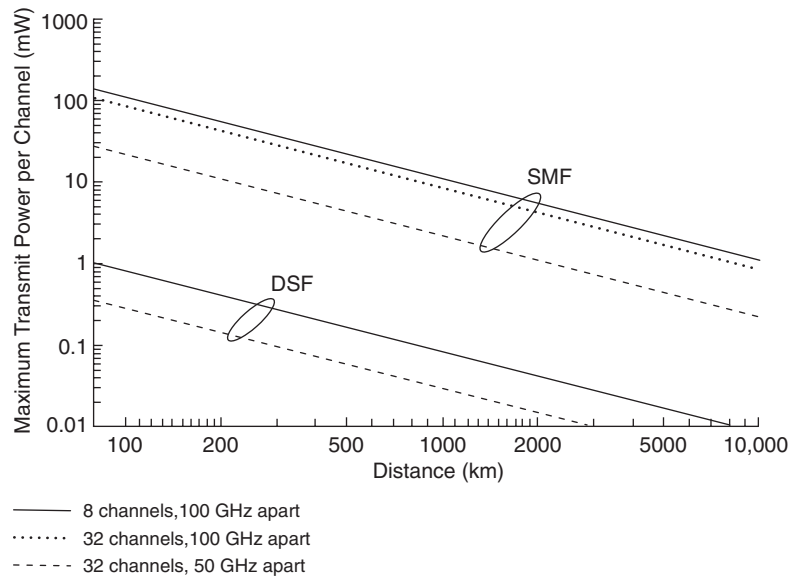


Fig. 5.30 Performance limitation imposed by the FWM process for two types of fiber and two classes of WDM systems.

Effective Area Fiber (LEAF) manufactured by Corning, Inc. has an area of $72 \mu\text{m}^2$; the True-wave XL Ocean fiber manufactured by OFS also offers the same effective area. The standard SMF has an effective area around $50 \mu\text{m}^2$. The Corning Vascade L1000 fiber offers an effective area of $101 \mu\text{m}^2$. Looking at research results, a fiber design using a novel approach claims an effective area of $1470 \mu\text{m}^2$ (Wong et al., 2005).

System design with optical nonlinearities present is a complex undertaking and after some preliminary calculations one has to use a simulation package that solves the nonlinear propagation equation (nonlinear Schrödinger equation) under the conditions imposed by the system details. A good introduction is given in Agrawal (2005).

Future Evolution of Optical Fiber Communications

Silica glass proved to be the ideal material in its optical and mechanical properties and also for manufacturing cabling and reliability. The losses have been reduced to such an extent that any further progress in that direction will be met with the law of diminishing returns. There has been work on new glass materials whose intrinsic theoretical losses are less than that of silica. They are collectively referred to as telluride and fluoride glasses. Figure 5.31 shows the theoretical loss spectrum of these glasses.

The interesting aspect of these losses is that, at the wavelengths where optical fiber systems operate now, silica glass is still as good as or better than these new glasses. Therefore, to exploit the theoretical low fluoride losses, the optical window has to shift to longer wavelengths. Here semiconductor optical devices will have difficulties delivering the performance one has come to expect in the C- and L-bands and around 1300 nm. In spite of the theoretical low losses, experimental work with fluoride material has not delivered

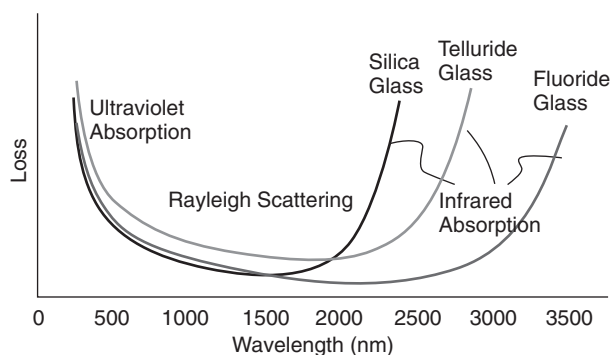


Fig. 5.31 Theoretical performance of some potential new fiber materials.

Source: FibreLabs, Inc. Used with permission.

results that will give confidence for the future. Therefore, from the material perspective, silica glass will continue to dominate the telecommunications market as far as one can see. As for multimode and single-mode fibers, the trend is to use single-mode fiber because it is future proof for bandwidth and its cost is low because it is manufactured in large volume. However, multimode fiber will keep a part of the market because of its special properties.

There was a time (late 1970s to late 1990s) when multimode fibers were considered obsolete on the grounds that operation in the fundamental waveguide mode provides better dispersion performance. However, it subsequently became apparent that there will be a huge market for optical LANs, data communications networks, and access networks. Multimode fibers offer greater ease of handling and splicing and therefore their role is being reevaluated, especially for cost-sensitive, short-span applications.

References

- Agrawal, G. P. (2001) *Nonlinear Fiber Optics*, Third Edition, Academic Press.
- Agrawal, G. P. (2005) *Lightwave Technology, Telecommunications Systems*, Wiley-Interscience.
- Buck, J. A. (2004) *Fundamentals of Optical Fibers*, Second Edition, John Wiley & Sons.
- Chigusa, Y., et al. (2005) Low-Loss Pure-Silica-Core Fibers and Their Possible Impact on Transmission Systems, *IEEE J. Lightw. Technol.* 23:3541–3450.
- Chraplyvy, A. R., et al. (1984) Optical Power Limits in Multi-Channel Wavelength Division Multiplexing, *Electron. Lett.* 20:58–59.
- Epworth, R. E. (1978) The phenomenon of modal noise in analogue and digital optical fibre systems, *Proceedings 4th European Conference on Optical Communications*, 492–501.
- Hecht, J. (1999) *City of Light: The Story of Fiber Optics*, Oxford University Press.
- Kao, K. C., and Hockman, G. A. (1966) Dielectric Fibre Surface Waveguides for Optical Frequencies, *Proceedings IEE* 113(July):1151–1158.
- Miya, T., Teramuna, Y., Hosaka, Y., and Miyashita, T. (1979) Ultra Low Loss Single Mode Fibre at 1.55 μm , *Electron. Lett.* 15:106–108.
- Ramaswami, R., and Sivarajan, K. (2002) *Optical Networks—A Practical Perspective*, Second Edition, Morgan Kaufmann.
- Senior, J. M. (1992) *Optical Fiber Communications*, Second Edition, Prentice Hall.
- Stolen, R. H. (1980) Nonlinearity in Fibre Transmission, *Proceedings IEEE* 68:1232–1236.
- Wong, W. S., et al. (2005) Breaking the Limit of Maximum Effective Area for Robust Single-Mode Propagation in Optical Fibers, *Opt. Lett.* 30:2855–2857.